



UNIVERSITY OF
BIRMINGHAM

Chaotic and Fractal Behaviour in Mathematical Billiards

Mike Knee

Issue: 1

Date: January 8, 2017

School of Physics and Astronomy
University of Birmingham
Birmingham, B15 2TT

Contents

1	Introduction	2
2	Basic Mathematical Billiards	2
2.1	Rectangular Table	2
2.2	Circular Table	3
2.3	Elliptical Table	4
2.4	Chaotic Behaviour	7
3	Complex Billiards Tables	10
3.1	Stadium Table	10
3.2	Lorentz Table	16
4	Fractal Behaviour	16
4.1	Fractal Dimensions	19
5	Conclusion	22
A	Reproducing Results	23
A.1	Basic Paths	23
A.2	Chaotic Behaviour	23
A.3	Fractals	23
A.4	Box Dimensions	24

1 Introduction

This project aims to investigate the properties of billiard ball trajectories over different table types in classical mathematical billiards. Mathematical billiards is a point particle moving across a table and colliding elastically with the walls of the table (I.e. with no velocity dissipation).

A number of different table types are to be investigated, starting with the straightforward rectangular, circular and elliptical shapes. These will be discussed briefly before exploring the more complicated stadium (or Bunimovich) and Lorentz tables.

The stadium table is a rectangular table capped with two semicircles, and produces chaotic results. The Lorentz table is a rectangular table with a circular portion removed from the centre. The stadium table will be discussed in detail, as it produces chaotic and possibly fractal results. The Lorentz table has properties relating to the ideal gas, which will be discussed briefly but is beyond the scope of this project.

2 Basic Mathematical Billiards

The basic interaction for all billiards tables are collisions with the boundary. These result in the angle of reflection being equal to the angle of incidence. All the tables studied in this report have no other properties (e.g. curvature) and so between collisions with the boundary the velocity of the billiard ball is constant.

Using this information it was possible to only compute collision points, and assume the ball takes straight-line paths between these collision points.

To compute the velocity after a ball has collided with the wall the formula

$$\mathbf{r} = \mathbf{i} - 2(\mathbf{i} \cdot \tilde{\mathbf{n}})\tilde{\mathbf{n}} \quad (1)$$

was used; where \mathbf{r} is the reflected vector (or final velocity), \mathbf{i} is the incident vector (or initial velocity) and $\tilde{\mathbf{n}}$ is the surface normal [2].

2.1 Rectangular Table

The rectangular table is the simplest table type. This table exhibits no chaotic properties, as will be demonstrated, and small changes in initial conditions do not create divergent paths. There are two types of possible path, periodic and non-periodic.

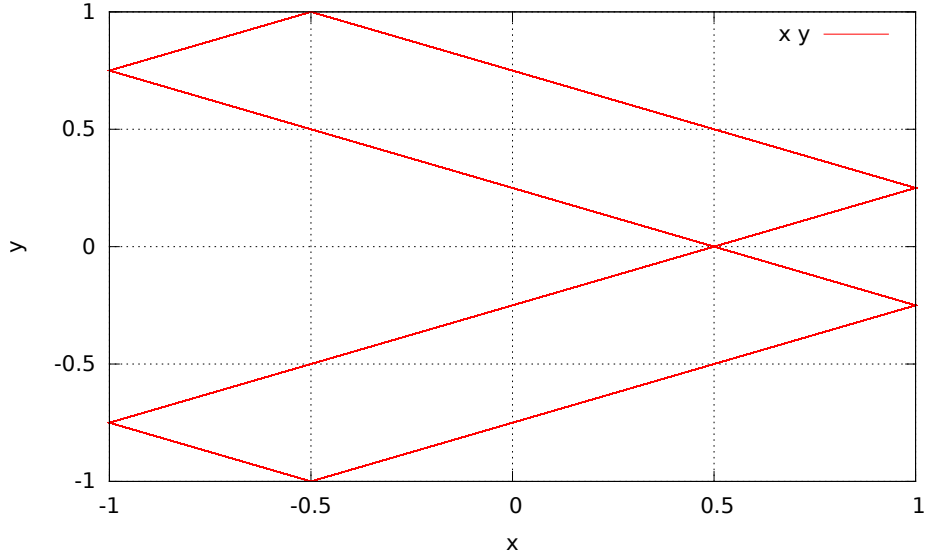


Figure 1: Periodic path on a rectangular table. Starting from $(0.5, 0)$ with velocity $(0.8, 0.2)$ with 1000 bounces.

When the billiard ball collides with the wall it's velocity is reflected in the normal of the wall. As the wall normals always lie along the x or y axes this means that one of the components of the velocity is negated and the other remains constant. I.e. on a collision with the right hand wall the y component of the velocity is unchanged and the x component is negated.

There is a special case when the ball collides with the corner of the table. In this simulation the corner collision was modelled as if the ball collided with both walls one after the other within an infinitely small period of time. The result of this is that both the x and y component of the velocity are negated.

Periodic paths, like the one in figure 1, are produced when the path trajectory has a rational slope (I.e. $v_y/v_x \in \mathbb{Q}$). See [1], chapter 1 for details.

Non-periodic paths can be produced by randomising the initial conditions for the billiard ball. (Again see [1].) Although the trajectory is not truly irrational, as the maximum precision of double variables is 15 significant figures (and not infinite as required for true irrational numbers) this nevertheless produces results that demonstrate the non-periodicity. Figure 2 demonstrates how random initial conditions produces non-periodicity.

2.2 Circular Table

The circular table, like the rectangular table produces either periodic or non-periodic paths. Periodic path examples are shown in 3. All regular polygons can be reconstructed as periodic paths of the circular table.

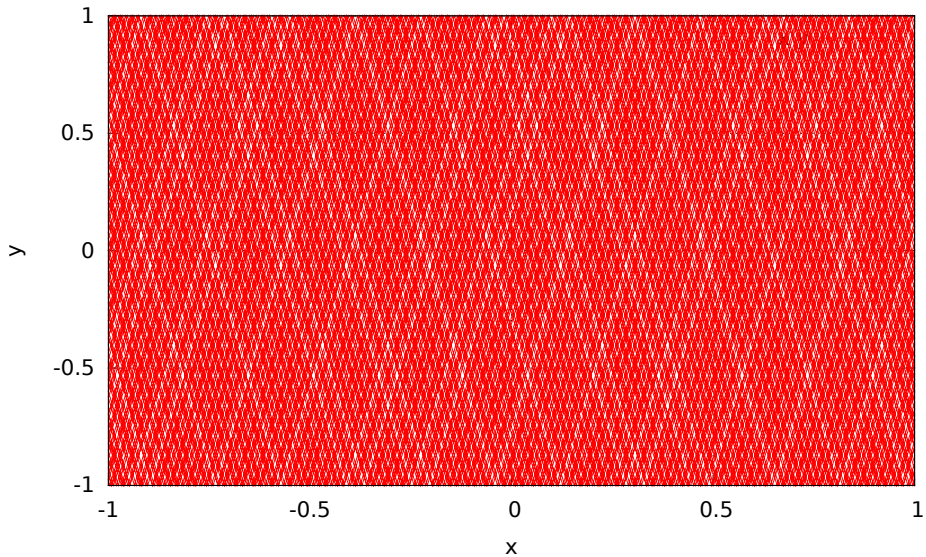


Figure 2: Non-periodic path on a rectangular table. Randomised initial conditions, with 1000 bounces.

Non-periodic paths can again be produced by randomising the initial conditions. These paths all have a "caustic", which is the inner circle bounded by the points on the path that lie closest to the centre of the billiards table.

Figure 4 shows a non-periodic path, with the caustic visible with a radius of about 0.5. The caustic represents the trajectory's closest approach to the centre of the circle.

2.3 Elliptical Table

The elliptical table behaves similarly to the circular table, with the possibility of producing either periodic or non-periodic paths.

The periodic paths are again given by polygons, though unlike in the circle they are no longer regular (see [6]). The major and minor axis of the ellipse are also periodic paths for the billiards ball.

The non-periodic paths display a caustic, but in the case of the ellipse this can either be a hyperbolic or elliptical caustic, depending on the initial conditions. Hyperbolic caustics are produced when the initial trajectory crosses the major axis between the two foci of the ellipse. An example of this kind of non-periodic behaviour is shown in figure 5.

Elliptical caustics are produced when the initial trajectory does not cross the major axis between the two foci (and does not pass through either of the two foci). An example of this is shown in figure 6.

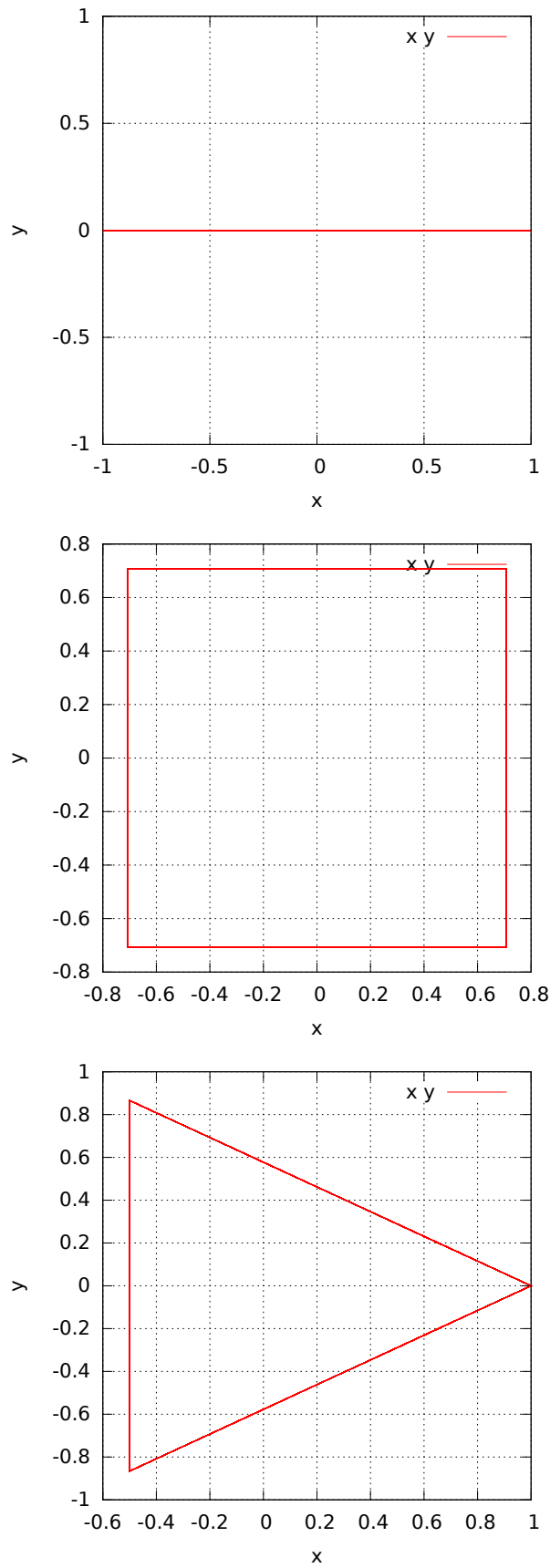


Figure 3: Periodic paths in a circular billiards table.
page 5 of 25

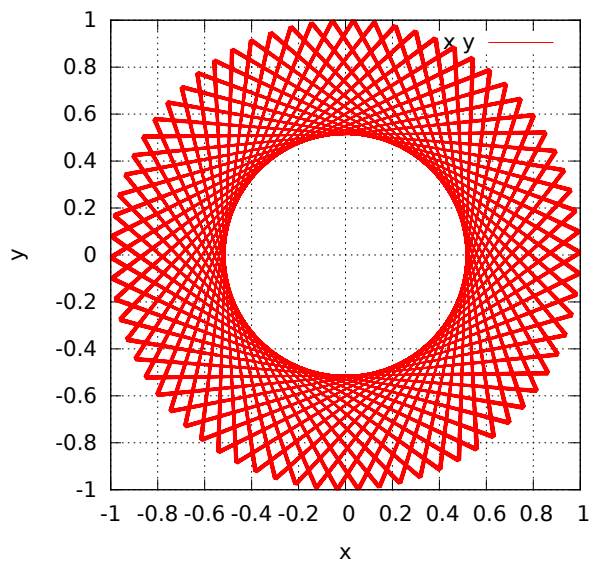


Figure 4: Non-periodic path of a billiard on a circular table. Randomised initial conditions with 1000 iterations.

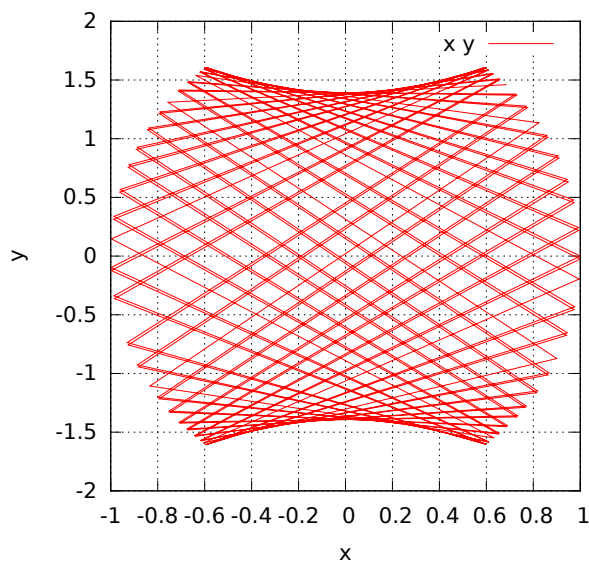


Figure 5: Elliptical table with randomised initial conditions, displaying a hyperbolic caustic.

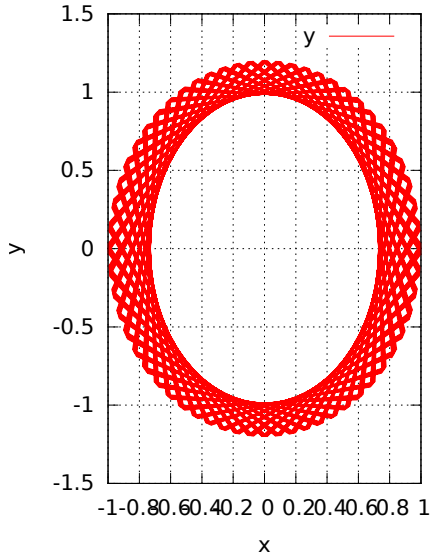


Figure 6: Elliptical table with randomised initial conditions, displaying an elliptical caustic.

The final possibility for the elliptical table is that the initial trajectory passes through one of the foci of the ellipse. In this case, at every subsequent reflection the trajectory will pass through one of the two foci. This creates a non-periodic trajectory, with each reflection producing a path that tends towards the major axis (I.e. tends towards passing through both foci). An example of this is shown in figure 7.

Here the table has been parametrised by the equation

$$x^2 + \left(\frac{y}{1.2}\right)^2 = 1 \quad (2)$$

and the focus is given by

$$f = \sqrt{a^2 - b^2} \quad (3)$$

so in this case the foci are at $\pm\sqrt{1.2^2 - 1} = 0.66332$.

2.4 Chaotic Behaviour

One of the properties of a chaotic system is small changes in initial conditions create very large and unpredictable changes as the system progresses. To examine this behaviour the simulation was run twice with very slight changes to initial conditions, and the state of the two systems after each iteration was compared. It was anticipated that none of these simple

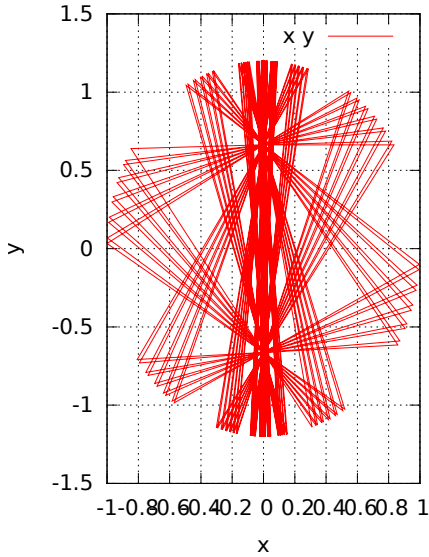


Figure 7: Elliptical table displaying a convergent non-periodic path. Initial position of the billiards ball is in this case the top focus of the ellipse.

billiards tables would exhibit chaotic behaviour, but for comparison and to demonstrate this the chaotic simulation was run.

To compare the state of the conditions the collision point angle was used. This angle corresponds to a unique position on the table circumference, and can be thought of as a way to parametrise the collision point. This parameter is referred to as θ through this chapter. The difference between the two systems is given by $\epsilon = |\theta_1 - \theta_2|$.

This measurement has a drawback, as θ has a maximum value of 2π . When θ goes above 2π it is given a value of θ modulo 2π , i.e. $\theta - 2\pi$. This can occasionally produce large jumps in the measurement of ϵ . These anomalies should be rare, however, and can often be isolated.

The rectangular table produces no divergence, with ϵ remaining constant no matter the difference in initial position input to the system. If instead the velocity is varied slightly a linear change in ϵ is shown 8. This linear divergence means that the rectangular billiards table is not a chaotic system.

For the circular table varying either the initial velocity or position also produce a linear change in ϵ , with figure 9 showing how the position difference diverges when the initial position is varied slightly. Again this billiards table does not display chaotic properties, as the divergence is linear.

The elliptical table does not produce linear changes in ϵ as in the circular and rectangular tables. In this case ϵ varies in a oscillatory nature, as shown by the graphs in figure 10. Varying either initial position or velocity produces this result.

This behaviour is caused by the elliptical or hyperbolic shape of the caustic. As the two

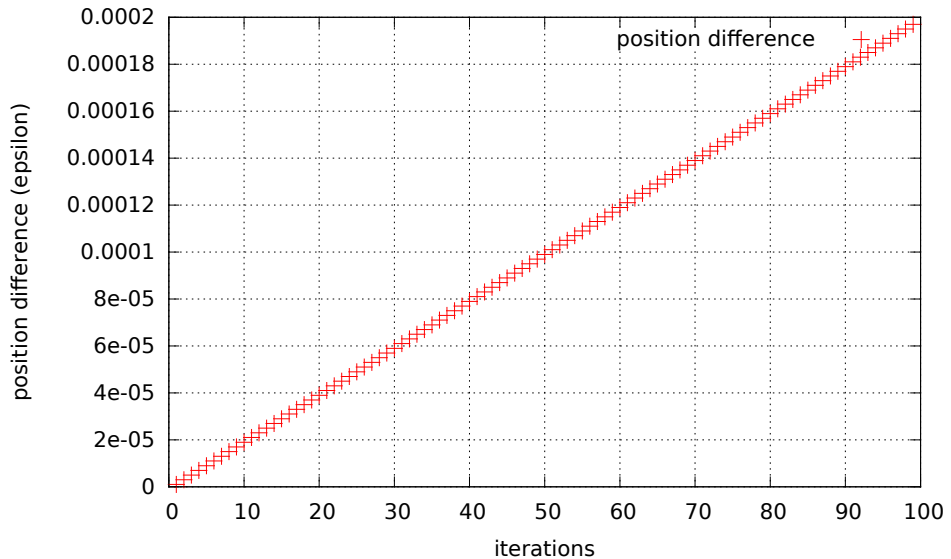


Figure 8: Divergence of two rectangular systems with small changes to initial velocity.

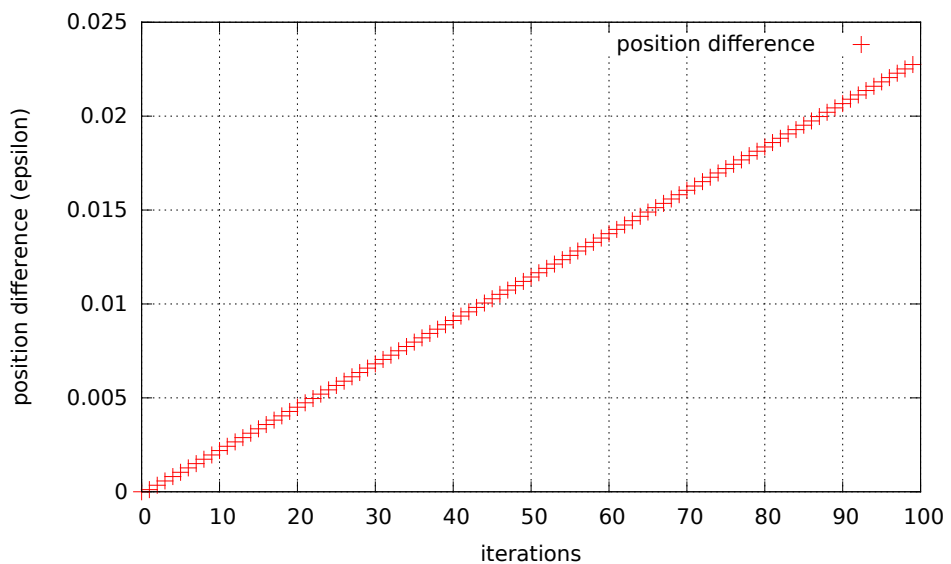


Figure 9: Divergence of two circular systems with slight changes to initial position.

systems reach the vertices furthest from the origin, where the curvature of the ellipse is at a maximum, the billiards ball's trajectories become very focused. This can be seen clearly in figure 5. As the two systems reach the other vertices, where the curvature is at a minimum, the opposite affect occurs. This creates the oscillatory behaviour in path difference.

However, this behaviour is not chaotic as a regular change in the position difference is observed. None of the simple billiards tables exhibit the chaotic behaviour, as was expected.

3 Complex Billiards Tables

The two complex billiard tables studied in this project are the stadium table and the lorentz table. The stadium table is a rectangle with two semi-circles attached at opposite ends. The lorentz table is a rectangle with a circle removed from the centre. Both these tables exhibit chaotic properties.

3.1 Stadium Table

The stadium table (figure 11) is a type of Bunimovich billiard table (see [1] chapter 8). The condition for a Bunimovich table is that every focusing arc (i.e. convex part of the boundary) is a circular arc, which can be completed to a full circle without crossing the table boundary. This is true for the stadium table, as both the semi-circles can be completed to full circles without crossing the boundary of the table. Other bunimovich tables are possible and also exhibit chaotic behaviour but are not covered in this project. [1] contains more information on different types of Bunimovich table.

Periodic paths can be produced on the stadium table. Any trajectory with initial velocity along the y axis, which starts in the rectangular section of the table, will produce a periodic path bouncing between the two straight wall sections of the table. Another periodic path can be produced by starting at any point on the x axis, and travelling with initial velocity along the x axis.

Other periodic paths can be produced in a similar manner to the circular regular polygon paths. Any path that creates a regular polygon with an even number of sides in a circular table can be modified to produce a 'stretched' version of the polygon on the stadium table. An example of the square periodic trajectory on a circular table recreated on the stadium table is shown in figure 12.

The chaotic nature of this table means that, unlike for the simpler table types, running the simulation for a higher number of iterations with the same initial conditions as would create a periodic path can result in a non-periodic path. This is because the initial variables are stored as double precision, and have a limit on the accuracy they can store numbers as. This small error propagates quickly and produces a non-periodic path, as seen in figure 13.

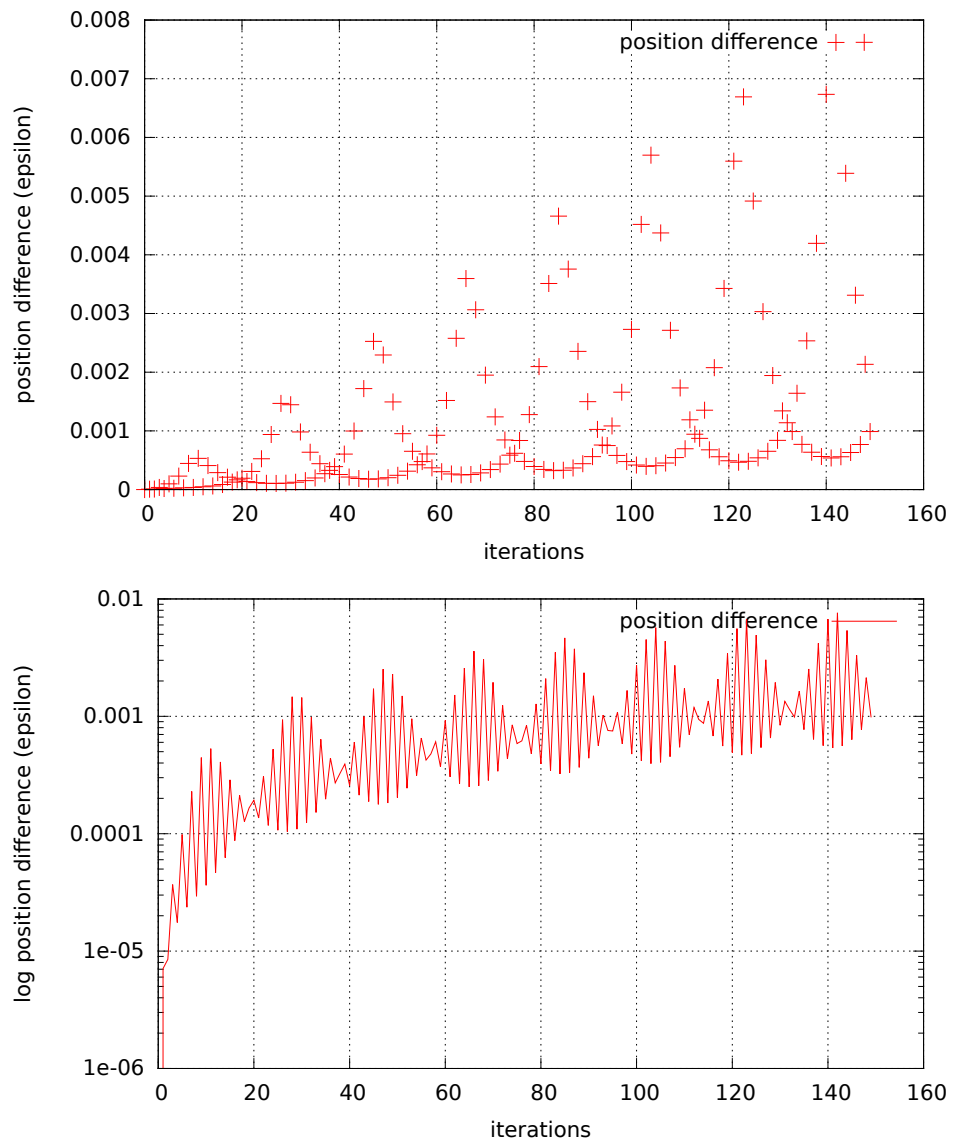


Figure 10: Position difference in an elliptical system with varying initial position, shown as a regular plot and as a log plot.

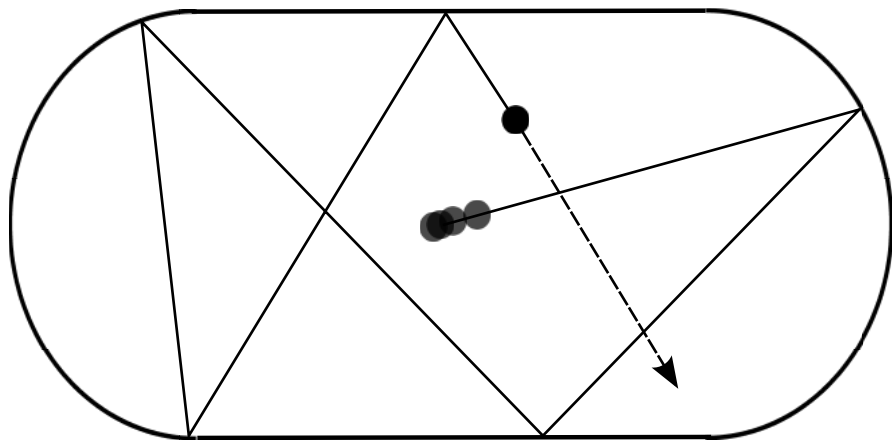


Figure 11: Stadium billiards table. [4]

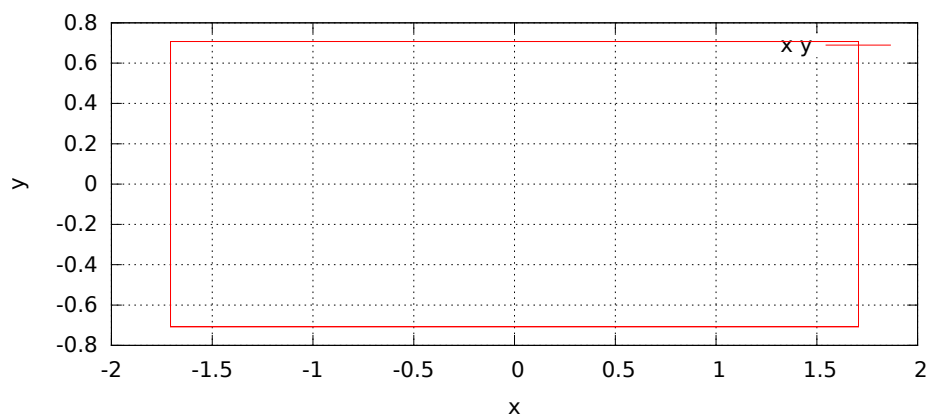


Figure 12: Rectangular periodic path on a stadium table (10 iterations).

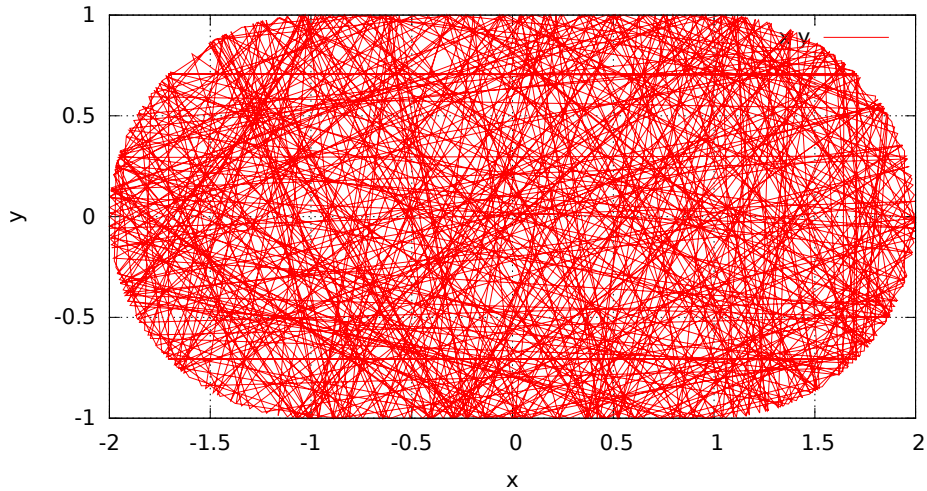


Figure 13: Non-periodic path, produced from the same initial conditions as the rectangular periodic path (500 iterations).

The way this error expands in this table compared to the simple tables like the circular table is due to a defocusing affect created by the circular arc portions of the table. Circular arcs focus trajectories onto a caustic (in the case of the trajectory passing through the circle centre the caustic is the centre point) but once the trajectory has passed the caustic it 'defocuses'. In a circular table it is only defocused as much as it was initially focused before it hits the boundary of the table again. However, in the stadium table this does not always occur, because of the straight line sections of the table. This causes the defocusing, and therefore chaotic behaviour of the table. ([1] chapter 8.2.)

The chaotic nature of this table can be investigated in a similar way to the simple tables. Here the chaotic behaviour of stadium tables with different dimensions were also analysed. First a stadium table with a very short rectangular section was analysed, and the results are shown in figure 14. For the first 60 iterations the position difference seems to be increasing a very small amount, in a manner similar to the non-chaotic simple tables. After this period the position difference starts to diverge by seemingly random amounts. This is indicative of true chaotic behaviour. There is also a nearly repeated pattern observed in the log path difference graph, this 'disordered order' is also typical of many chaotic systems.

Next a stadium table with a square rectangular section was analysed. The results are shown in figure 15. If we compare it to the previous stadium table we can see that the chaotic affect becomes evident after only around 10 iterations compared to the 60 previously. We also see less of the disordered order, and the position difference in the chaotic section appears to be totally random.

These graphs show that even a very small rectangular section in the stadium table produces chaotic behaviour, and that if we change the dimensions to a square rectangular section the

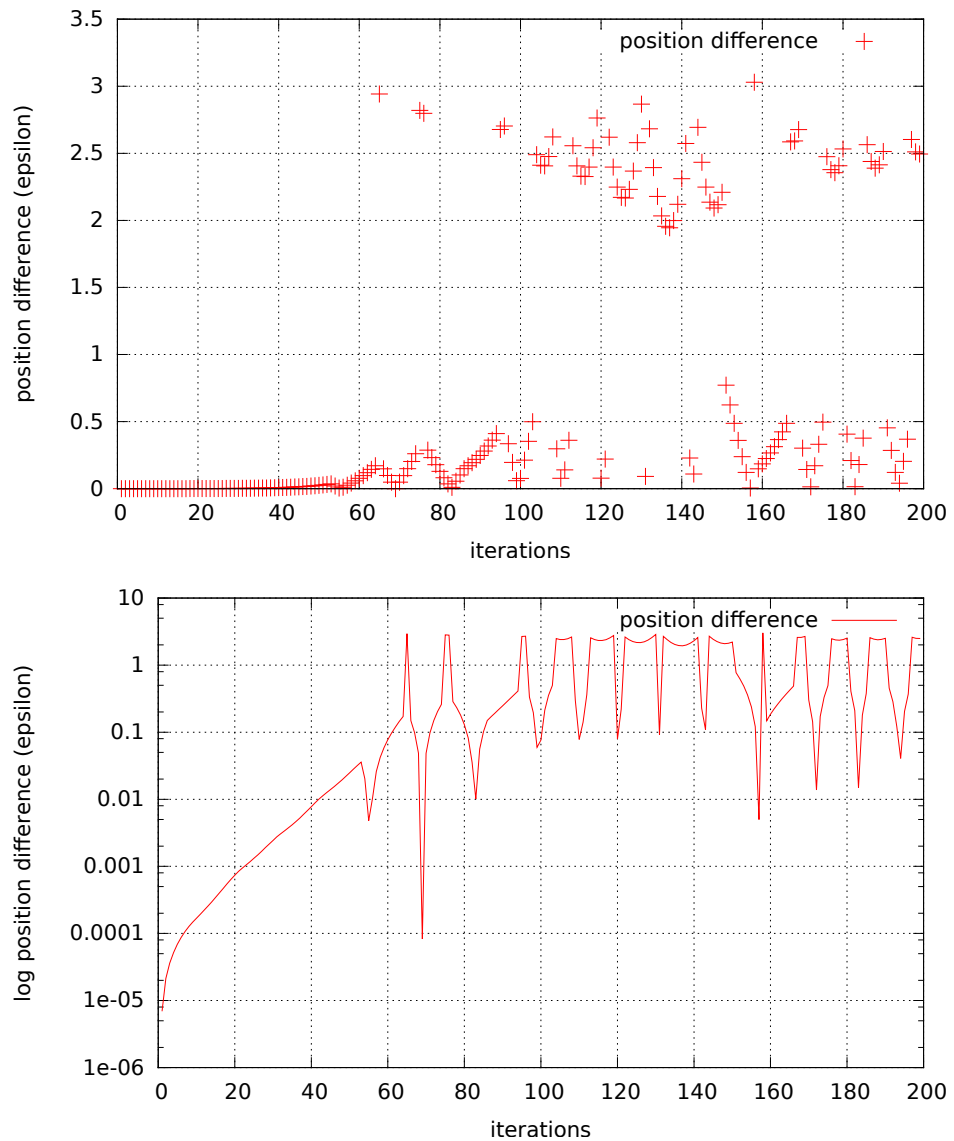


Figure 14: Path difference for a stadium table with a very short rectangular section (0.02 rectangular section, 1 semi-circle radius).

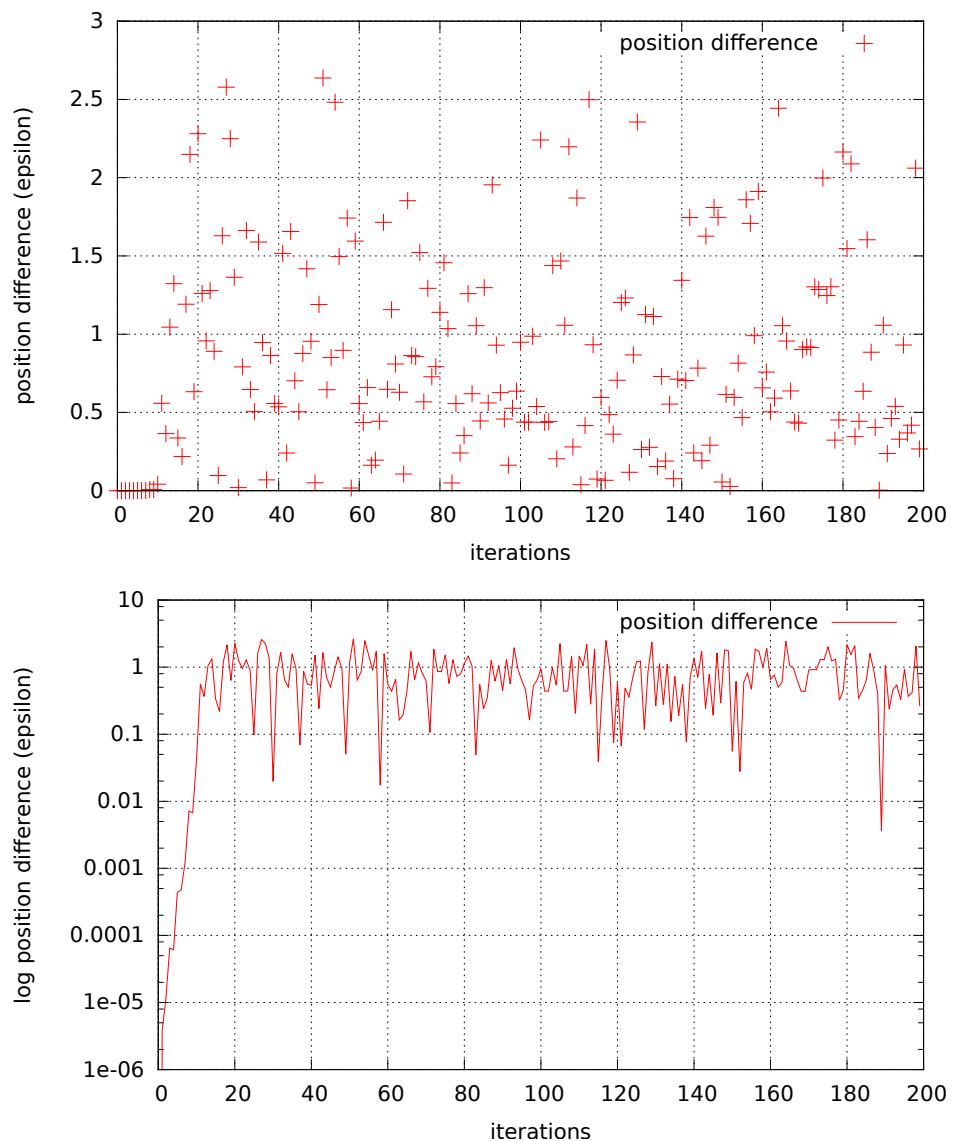


Figure 15: Path difference for a stadium table with a square rectangular section (2 rectangular section, 1 semi-circle radius).

chaotic affect becomes stronger, with paths diverging very quickly.

3.2 Lorentz Table

The Lorentz table (figure 16) is representative of the Lorentz gas. The central circle models the stationary atoms in a lattice, and the billiard ball models an electron. In order to recreate the actual trajectory the path must be "unfolded" every time the billiard hits the outer wall of the table, as shown in figure 17. This model is constrained to only two dimensions, but an extension to three dimensions is possible.

This table is expected to produce chaotic results, due to the defocusing affect of the convex central circular portion of the table.

Periodic paths are possible on the table, most of which correspond to periodic paths on the rectangular table which do not collide with the central circle. This means the radius of the central circle affects whether certain trajectories will produce periodic paths or not. Other periodic paths correspond to the billiard starting on one of the axis and travelling with initial velocity along that axis. Along with these axis periodic paths there are four other possible periodic paths corresponding to the billiard starting on the lines $y = x$ or $y = -x$ and travelling along these lines. This allows the billiard to reflect at the corner, and then hit the central ball with a 0 angle of incidence.

Chaotic behaviour analysis was performed on the Lorentz table, and the results are shown in figure 18. If these graphs are compared to the results for the stadium table in figure 15 the chaotic behaviour of both tables is clear. The graphs display all the same features and indicate that the lorentz table also has chaotic properties.

4 Fractal Behaviour

Using the chaotic table types it should be possible to produce fractal plots in certain phase spaces. The phase space chosen to produce these images in this project was the initial velocity angle plotted against the total distance travelled. This is plotted radially, as the radial nature of the initial velocity angle lends itself to this coordinate system. To produce this plot each run of the simulation starts in the same place, which is next to the right wall of the table offset by a set amount (in most cases 0.00001).

The main two properties of a fractal are self similarity and non-integer dimensions [3]. Self-similarity can only be qualitatively estimated, but the dimensions of the produced images can be measured using the box-dimension method which will be discussed in section 4.1.

The stadium table plot is shown in figure 19. This figure is a zoom of the original plot, which is not included here as any of the important features cannot be easily made out. From

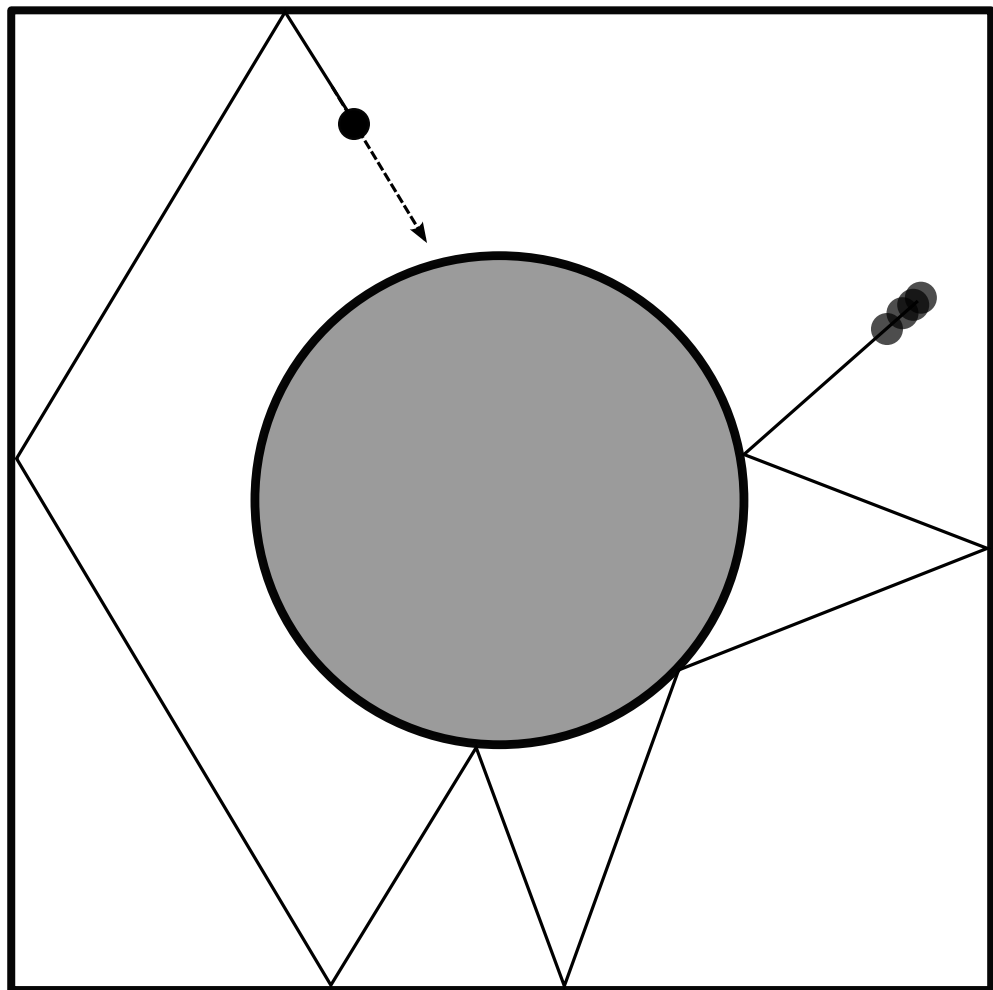


Figure 16: Lorentz billiards table. [5]

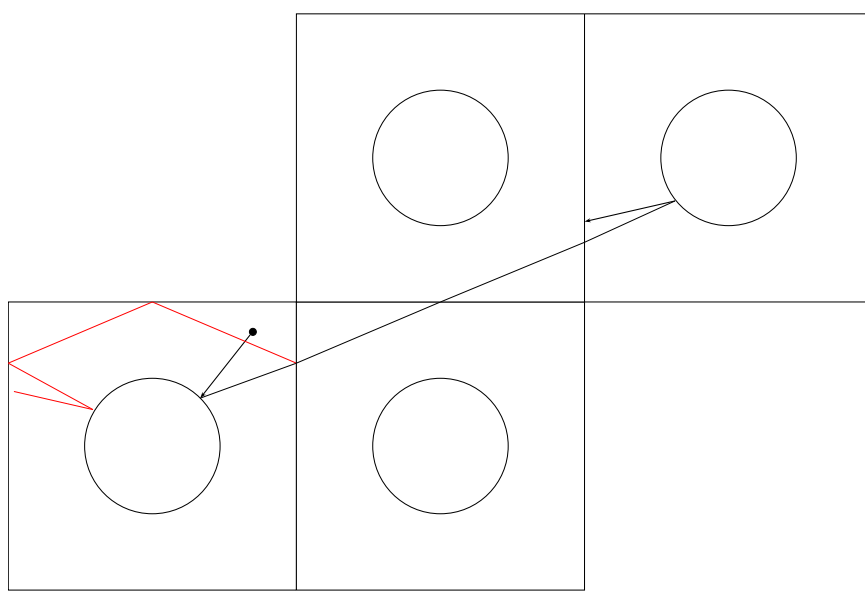


Figure 17: Unfolding the trajectory of a billiards ball on a Lorentz table.

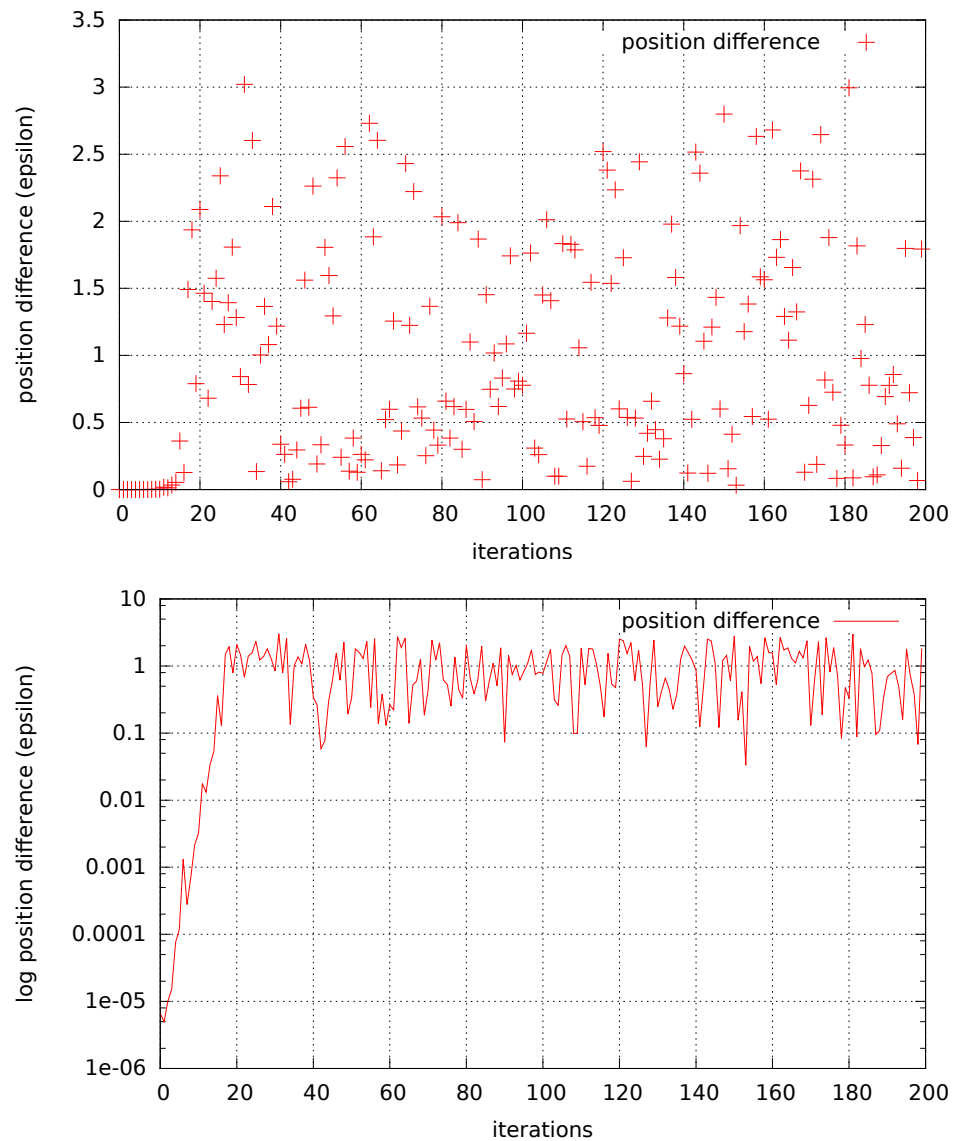


Figure 18: Path difference for a lorentz table with an inner circle radius 1 and a square rectangular section, side length 4.

looking at the plot some evidence of self-similarity is apparent, however this is not enough to justify calling this plot a fractal with certainty.

The lorentz table plot is shown in figure 20. Self-similarity also appears to be present in this phase plot, but again further investigation is required before the fractal nature of this image can be determined.

4.1 Fractal Dimensions

In order to measure the fractal dimension of these images a technique known as box-counting or the MinkowskiBouligand dimension was investigated. This method involves placing a grid over the image, and counting how many of the boxes are needed to cover the image. By varying the size of the grid squares and observing how this affects the number of boxes needed to cover the image the box dimension can be calculated.

If the image is overlayed with a grid with box side length ϵ the box dimension is given by

$$D = \lim_{\epsilon \rightarrow 0} \frac{\log N(\epsilon)}{\log 1/\epsilon} \quad (4)$$

where N is the number of boxes needed to cover the image. To compute D a script was written to take in the data used to plot the radial phase plots in figures 19 and 20 and count the number of points in varying grid square sizes.

Because of the time intensive nature of this box counting script only 100 different initial angles were generated, compared to the 10000 used in the fractal figures.

$\log N$ was plotted against $\log 1/\epsilon$ for the stadium table and the results are shown in figure 21. The box dimension is given by the slope of this graph. As the box length decreases the log number of occupied squares increases. Between 0.1 and 1 $\log 1/\epsilon$ the slope of the graph begins to decrease, and it appears to be converging towards 0 as the box length increases.

At the top end of the graph the gradient of the curve appears to be approaching 0. This is because instead of a line image simple points are being analysed. This means as we get to very small box sizes each box can only cover one point and the number of occupied squares no longer increases. This means the box dimension calculation used here is not accurate enough, and cannot conclusively show whether the images generated are fractal.

If instead the images were generated using line plots and analysed using image processing techniques it may be possible to generate a more accurate estimation of the box dimension. Using a higher number of points in the analysed data may also increase the accuracy of this analysis, but any meaningful increase in the number of initial angles causes a large increase in time taken to run. The algorithm runs exponentially and an increase to 1000 points is estimated to take up to several days to run completely. For this reason this analysis has not

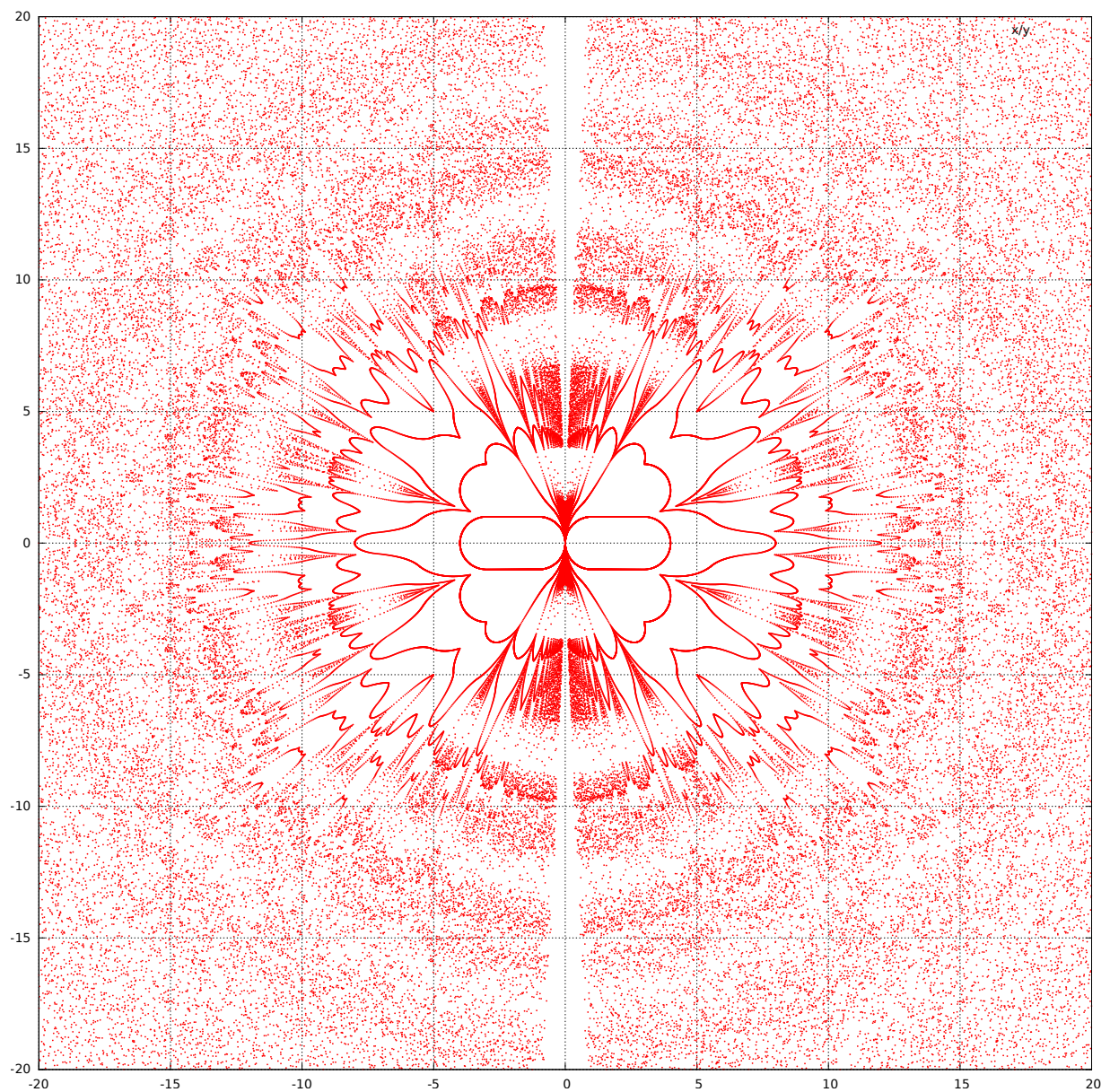


Figure 19: Zoomed radial phase plot of initial velocity angle against total path length for the stadium table. θ corresponds to initial velocity angle, r to total distance travelled. 30 iterations at each initial velocity angle.

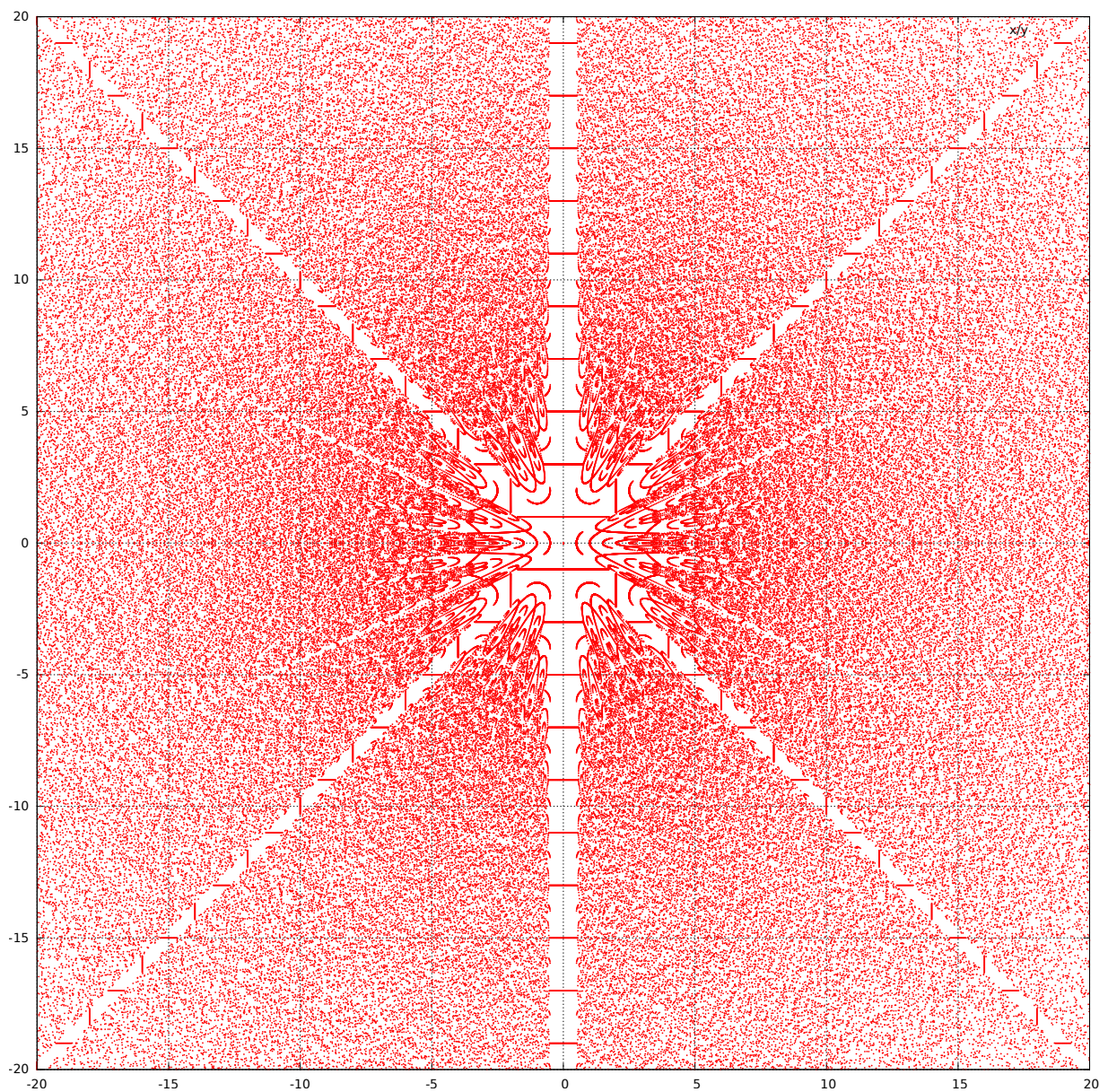


Figure 20: Zoomed radial phase plot of initial velocity angle against total path length for the Lorentz table. θ corresponds to initial velocity angle, r to total distance travelled. 30 iterations at each initial velocity angle.

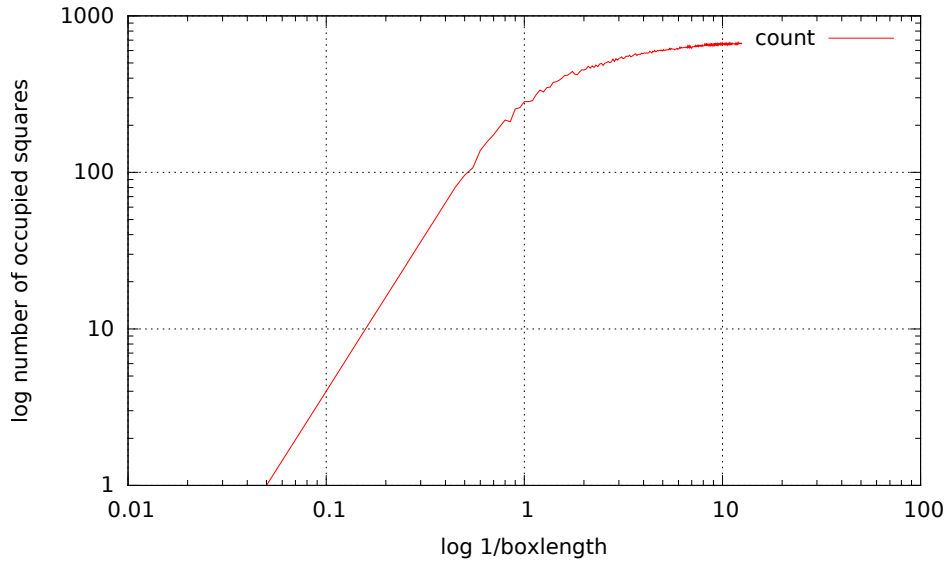


Figure 21: Box dimension data for the stadium table.

been performed.

5 Conclusion

In this project the properties of different mathematical billiards tables were explored. The goal was to investigate the chaotic and fractal properties of complex billiard tables, such as the stadium billiards table.

The chaotic properties of different table shapes have been thoroughly investigated in this report. The simple tables have been shown to have no chaotic properties, whereas the more complicated billiard tables (the stadium and lorentz tables) have strongly chaotic properties. Of note is the way the chaotic features of the stadium table become more pronounced the further away from the basic circular table the stadium gets (i.e. the longer the rectangular section).

The fractal properties of the complex tables have been investigated, however the box dimension analysis has proved inconclusive and remains a possibility for further study. The phase plots generated appear to be fractal in nature (exhibiting self-similarity) however without a good measure of the fractal dimension there is no way to verify this property.

A Reproducing Results

To reproduce the data and graphs contained within this report one can use the accompanying analysis scripts included alongside the source code and final executable of the billiard simulation.

A description of how to use these scripts to generate the graphs included in the report is included here for completeness.

A.1 Basic Paths

The basic path plots, such as the ones in figures 4 and 13 are generated by first creating data using the “regular plot” option in the billiards simulation. This will create a data file named `<TABLE_TYPE>out.dat`. This can be passed to the plotting script `plotter`, and a set of graphs will be automatically generated. The only graph of note is the one called `path.pdf`, the others are different phase space plots that proved to not be relevant to this report.

The report contains details as to the initial conditions needed to generate the graphs exhibiting different properties. In general the non-periodic properties can be shown by choosing the random initial conditions. (It would be highly unlikely that a periodic path would be generated if random initial conditions were picked.)

A.2 Chaotic Behaviour

The chaotic behaviour analysis is performed by selecting the “chaotic behaviour” option in the billiards simulation, creating a data file named `chao<TABLE_TYPE>out.dat`. This can then be passed to the plotting script and the correct graph types will be selected. The data file must start with the 4 characters `chao` in order for the plotting script to correctly identify the data type.

The script will produce two `.pdf` output files, one of which shows the divergence and the other the log divergence after each iteration.

A.3 Fractals

As before the “fractal plot” option must be selected in the simulation. The resulting data file can then be passed to the plotting script. In this case three pdf output files will be created. The ones used in the report are called `radialDistanceAngle.pdf`.

It may be useful to tweak the inner `.plot.pgi` file (which contains the commands that gnuplot uses to generate the graphs) at this point. Lines 19 and 20 in this file dictate the zoom

of the radial fractal plot. The x and y range used in the report is $-20, 20$ but this could be modified to produce more or less zoomed graphs when the script is run.

A.4 Box Dimensions

The script `DimensionCalculator.py` was used to generate box dimensions data from the fractal data created by the simulation. It outputs to `boxdim.dat`, which as before can be passed to the plotting script to generate graphs.

This script will run in exponential time, and outputs the step it is on at each iteration to see the progress. Running this with a high number of boxes, or with a high resolution fractal data set will take an extremely long time, and is not recommended.

References

- [1] N. Chernov and R. Markarian. *Chaotic Billiards*. Mathematical surveys and monographs. American Mathematical Society, 2006. ISBN: 9780821840962. URL: <https://books.google.co.uk/books?id=Zu5u7wfHstsC>.
- [2] Phrogz (<http://math.stackexchange.com/users/4241/phrogz>). *How to get a reflection vector?* Mathematics Stack Exchange. eprint: <http://math.stackexchange.com/q/13263>. URL: <http://math.stackexchange.com/q/13263>.
- [3] Edyta Patrzalek. *Fractals: Useful Beauty*. Visited on: 05/01/2017. URL: <http://www.fractal.org/Bewustzijns-Besturings-Model/Fractals-Useful-Beauty.htm>.
- [4] George Stamatiou. *BunimovichTable*. Visited on: 05/01/2017. July 2009. URL: <https://commons.wikimedia.org/wiki/File:BunimovichStadium.svg>.
- [5] George Stamatiou. *SinaiBilliard*. Visited on: 05/01/2017. Apr. 2009. URL: <https://commons.wikimedia.org/wiki/File:SinaiBilliard.svg>.
- [6] Eric W. Weisstein. *Billiards*. Visisted on: 01/01/2017. URL: <http://mathworld.wolfram.com/Billiards.html>.